



Observation of CP violation in $B^\pm \rightarrow DK^\pm$ decays[☆]

LHCb Collaboration

ARTICLE INFO

Article history:

Received 19 March 2012
Received in revised form 19 April 2012
Accepted 25 April 2012
Available online 30 April 2012
Editor: W.-D. Schlatter

Keywords:

LHC
 CP violation
Hadronic B decays

ABSTRACT

An analysis of $B^\pm \rightarrow DK^\pm$ and $B^\pm \rightarrow D\pi^\pm$ decays is presented where the D meson is reconstructed in the two-body final states: $K^\pm\pi^\mp$, K^+K^- and $\pi^+\pi^-$. Using 1.0 fb^{-1} of $\sqrt{s} = 7 \text{ TeV}$ pp collisions, measurements of several observables are made including the first observation of the suppressed mode $B^\pm \rightarrow [\pi^\pm K^\mp]_D K^\pm$. CP violation in $B^\pm \rightarrow DK^\pm$ decays is observed with 5.8σ significance.

© 2012 CERN. Published by Elsevier B.V. Open access under CC BY-NC-ND license.

1. Introduction

A fundamental feature of the Standard Model and its three quark generations is that all CP violation phenomena are the result of a single phase in the CKM quark-mixing matrix [1]. The validity of the theory may be tested in several ways, and one – verifying the unitarity condition $V_{ud}V_{ub}^* + V_{cd}V_{cb}^* + V_{td}V_{tb}^* = 0$ – is readily applicable to B mesons. This condition describes a triangle in the complex plane whose area is proportional to the amount of CP violation in the theory [2]. Following the observation of CP violation in the B^0 system [3], the focus has turned to testing the unitarity of the theory by over-constraining the sides and angles of this triangle. Most related measurements involve loop or box diagrams, and for which the CKM mechanism is typically assumed when interpreting data [4]. This means the least-well determined observable, the phase $\gamma = \arg(-V_{ud}V_{ub}^*/V_{cd}V_{cb}^*)$ is of particular interest as $\gamma \neq 0$ can produce direct CP violation in tree decays.

Some of the most powerful methods for determining γ are measurements of the partial widths of $B^\pm \rightarrow DK^\pm$ decays where the D signifies a D^0 or \bar{D}^0 meson. In this case, the amplitude for the $B^- \rightarrow D^0 K^-$ contribution is proportional to V_{cb} whilst the $B^- \rightarrow \bar{D}^0 K^-$ amplitude depends on V_{ub} . If the D final state is accessible for both D^0 and \bar{D}^0 mesons, the interference of these two processes gives sensitivity to γ and may exhibit direct CP violation. This feature of open-charm B^- decays was first recognised in its application to CP eigenstates, such as $D \rightarrow K^+K^-$, $\pi^+\pi^-$ [5] but can be extended to other decays, e.g. $D \rightarrow \pi^-K^+$. This second category, labelled “ADS” modes in reference to the authors of [6], requires the favoured, $b \rightarrow c$ decay to be followed by a doubly Cabibbo-suppressed D decay, and the suppressed $b \rightarrow u$ decay

to precede a favoured D decay. The amplitudes of such combinations are of similar total magnitude and hence large interference can occur. For both the CP -mode and ADS methods, the interesting observables are partial widths and CP asymmetries.

In this Letter, we present measurements of the B^\pm decays in the CP modes, $[K^+K^-]_D h^\pm$ and $[\pi^+\pi^-]_D h^\pm$, the suppressed ADS mode $[\pi^\pm K^\mp]_D h^\pm$ and the favoured $[K^\pm\pi^\mp]_D h^\pm$ combination where h indicates either pion or kaon. Decays where the bachelor – the charged hadron from the B^- decay – is a kaon carry greater sensitivity to γ . $B^- \rightarrow D\pi^-$ decays have some limited sensitivity and provide a high-statistics control sample from which probability density functions (PDFs) are shaped. In total, 13 observables are measured: three ratios of partial widths

$$R_{K/\pi}^f = \frac{\Gamma(B^- \rightarrow [f]_D K^-) + \Gamma(B^+ \rightarrow [f]_D K^+)}{\Gamma(B^- \rightarrow [f]_D \pi^-) + \Gamma(B^+ \rightarrow [f]_D \pi^+)}, \quad (1)$$

where f represents KK , $\pi\pi$ and the favoured $K\pi$ mode, six CP asymmetries

$$A_h^f = \frac{\Gamma(B^- \rightarrow [f]_D h^-) - \Gamma(B^+ \rightarrow [f]_D h^+)}{\Gamma(B^- \rightarrow [f]_D h^-) + \Gamma(B^+ \rightarrow [f]_D h^+)}, \quad (2)$$

and four charge-separated partial widths of the ADS mode relative to the favoured mode

$$R_h^\pm = \frac{\Gamma(B^\pm \rightarrow [\pi^\pm K^\mp]_D h^\pm)}{\Gamma(B^\pm \rightarrow [K^\pm\pi^\mp]_D h^\pm)}. \quad (3)$$

Elsewhere, similar analyses have established the $B^\pm \rightarrow D_{CP} h^\pm$ modes [7–9] and found evidence of the $B^\pm \rightarrow [\pi^\pm K^\mp]_D K^\pm$ decay [10–12]. Analyses of $B^\pm \rightarrow [K_S^0 \pi^+ \pi^-]_D K^\pm$ decays [13,14] have yielded the most precise measurements of γ though a 5σ observation of CP violation from a single analysis has not been achieved. This work represents the first simultaneous analysis of

[☆] © CERN for the benefit of the LHCb Collaboration.

$B^\pm \rightarrow D_{CP}h^\pm$ and $B^\pm \rightarrow D_{\text{ADS}}h^\pm$ modes. It is motivated by the future extraction of γ which, with this combination, may be determined with minimal ambiguity.

This Letter describes an analysis of 1.0 fb^{-1} of $\sqrt{s} = 7 \text{ TeV}$ data collected by LHCb in 2011. The 2010 sample of 35 pb^{-1} is used to define the selection criteria in an unbiased manner. The LHCb experiment [15] takes advantage of the high $b\bar{b}$ and $c\bar{c}$ cross sections at the Large Hadron Collider to record large samples of heavy hadron decays. It instruments the pseudorapidity range $2 < \eta < 5$ of the proton–proton (pp) collisions with a dipole magnet and a tracking system which achieves a momentum resolution of 0.4–0.6% in the range 5–100 GeV/c. The dipole magnet can be operated in either polarity and this feature is used to reduce systematic effects due to detector asymmetries. In 2011, 58% of data were taken with one polarity, 42% with the other. The pp collisions take place inside a silicon microstrip vertex detector that provides clear separation of secondary B vertices from the primary collision vertex (PV) as well as discrimination for tertiary D vertices. Two ring-imaging Cherenkov (RICH) detectors with three radiators (aerogel, C_4F_{10} and CF_4) provide dedicated particle identification (PID) which is critical for the separation of $B^- \rightarrow DK^-$ and $B^- \rightarrow D\pi^-$ decays.

A two-stage trigger is employed. First a hardware-based decision is taken at a frequency up to 40 MHz. It accepts high transverse energy clusters in either an electromagnetic calorimeter or hadron calorimeter, or a muon of high transverse momentum (p_T). For this analysis, it is required that one of the three tracks forming the B^\pm candidate points at a deposit in the hadron calorimeter, or that the hardware-trigger decision was taken independently of these tracks. A second trigger level, implemented entirely in software, receives 1 MHz of events and retains $\sim 0.3\%$ of them. It searches for a track with large p_T and large impact parameter (IP) with respect to the PV. This track is then required to be part of a secondary vertex with a high p_T sum, significantly displaced from the PV. The displaced vertex is selected, with $\sim 75\%$ efficiency, by an online decision tree algorithm that uses p_T , χ_{IP}^2 , flight distance and vertex quality information of the B^\pm candidate. Full event reconstruction occurs offline, and after preselection around 2.5×10^5 events are available for final analysis.

Approximately one million simulated events for each $B^\pm \rightarrow [h^+h^-]_D h^\pm$ signal mode are used as well as a large inclusive sample of generic $B \rightarrow DX$ decays. These samples are generated using a tuned version of PYTHIA [16] to model the pp collisions. EVTGEN [17] encodes the particle decays and GEANT4 [18] describes interactions in the detector. Although the shapes of the signal peaks are determined directly on data, the inclusive sample assists in the understanding of the background. The signal samples are used to estimate the relative efficiency in the detection of modes that differ only by the bachelor track flavour.

2. Event selection

Sixteen combinations of $B^\pm \rightarrow Dh^\pm$, $D \rightarrow h^\pm h^\mp$ are formed where each h can be either a pion or a kaon. The candidate D meson mass must be within 1765–1965 MeV/c^2 to be accepted. D daughter tracks are required to have $p_T > 250 \text{ MeV}/c$ but this requirement is tightened to $0.5 < p_T < 10 \text{ GeV}/c$ and $5 < p < 100 \text{ GeV}/c$ for bachelor tracks to ensure best pion versus kaon discrimination. The decay chain is refitted [19] constraining the vertices to points in space and the D candidate to its nominal mass, $m_{\text{PDG}}^{D^0}$ [20].

Reconstructed candidates are selected using a boosted decision tree (BDT) discriminator [21]. It is trained using a simulated sample of $B^\pm \rightarrow [K^\pm \pi^\mp]_D K^\pm$ and background events from the

D -mass sideband ($35 < |m(hh) - m_{\text{PDG}}^{D^0}| < 100 \text{ MeV}/c^2$) of the independent sample collected in 2010. The BDT uses the following properties of the candidate B^\pm decay:

- From the tracks, the D and B^\pm : p_T and χ_{IP}^2 with respect to the PV;
- From the B^\pm and D : decay time, flight distance from the PV and vertex quality;
- From the B^\pm : the angle between the momentum vector and a line connecting the PV to its decay vertex.

Information from the rest of the event is employed via an isolation variable that considers the imbalance of p_T around the B^\pm candidate,

$$A_{p_T} = \frac{p_T(B) - \sum_n p_T}{p_T(B) + \sum_n p_T}, \quad (4)$$

where the $\sum_n p_T$ sums over the n tracks within a cone around the candidate excluding the three signal tracks. The cone is defined by a circle of radius 1.5 in the plane of pseudorapidity and azimuthal angle (measured in radians). The signal B decay tends to be more isolated with greater p_T asymmetry than combinatorial background. As no PID information is used as part of the BDT, it performs equally well for all modes considered here.

The optimal cut value on the BDT response is chosen by considering the combinatorial background level (b) in the invariant mass distribution of favoured $B^\pm \rightarrow [K\pi]_D \pi^\pm$ candidates. The large signal peak in this sample is scaled to the anticipated ADS-mode branching fraction to provide a signal estimate (s). The quantity $s/\sqrt{s+b}$ serves as an optimisation metric. The BDT response peaks towards 0 for background and 1 for signal. The optimal cut is found to be > 0.92 for the ADS mode; this is also applied to the favoured mode. For the cleaner CP modes, a cut of BDT > 0.80 gives a similar background level but with a 20% higher signal efficiency.

PID information is quantified as differences between the logarithm of likelihoods, $\ln \mathcal{L}_h$, under different particle hypotheses (DLL). Daughter kaons of the D meson are required to have $\text{DLL}_{K\pi} = \ln \mathcal{L}_K - \ln \mathcal{L}_\pi > 2$ and daughter pion must have $\text{DLL}_{K\pi} < -2$. Multiple candidates are arbitrated by choosing the candidate with the best-quality B^\pm vertex; only 26 events in the final sample of 157927 require this consideration.

The number of candidates from B decays that do not contain a true D meson can be reduced by requiring the flight distance significance of the D candidate from the B^- vertex to be > 2 . The effectiveness of this cut is monitored in the D sideband where it is seen to remove significant structures peaking near the B^- mass. A simulation study of the $B^- \rightarrow K^- K^+ K^-$, $K^- \pi^+ \pi^-$ and $K^- K^+ \pi^-$ modes suggests this cut leaves 2.5, 1.3 and 0.8 events respectively under the $B^- \rightarrow [K^+ K^-]_D K^-$, $[\pi^+ \pi^-]_D K^-$ and $[\pi^+ K^-]_D K^-$ signals. This cut also removes cross feed (e.g. $B^- \rightarrow [K^- \pi^+]_D \pi^-$ as a background of $[\pi^+ \pi^-]_D K^-$) which occurs when the bachelor is confused with a D daughter for events with a low D decay time. Finally, the combination of the bachelor track and the D -daughter track of opposite charge is made under the hypothesis both tracks are muons. The parent B candidate is vetoed if the invariant mass of this combination is within $\pm 22 \text{ MeV}/c^2$ of either the J/ψ or $\psi(2S)$ mass [20].

Due to misalignment, the reconstructed B^\pm mass is not identical to the established value, $m_{\text{PDG}}^{B^\pm}$ [20]. As simulation is used to define background shapes, it is useful to apply linear momentum scaling factors separately to the two polarity datasets so the B^\pm mass peak is closer to $m_{\text{PDG}}^{B^\pm}$. After this correction, the $D^0 \rightarrow K^- \pi^+$ mass peak is measured at 1864.8 MeV/c^2 with a resolution of 7.4 MeV/c^2 . Selected D candidates are required to be within

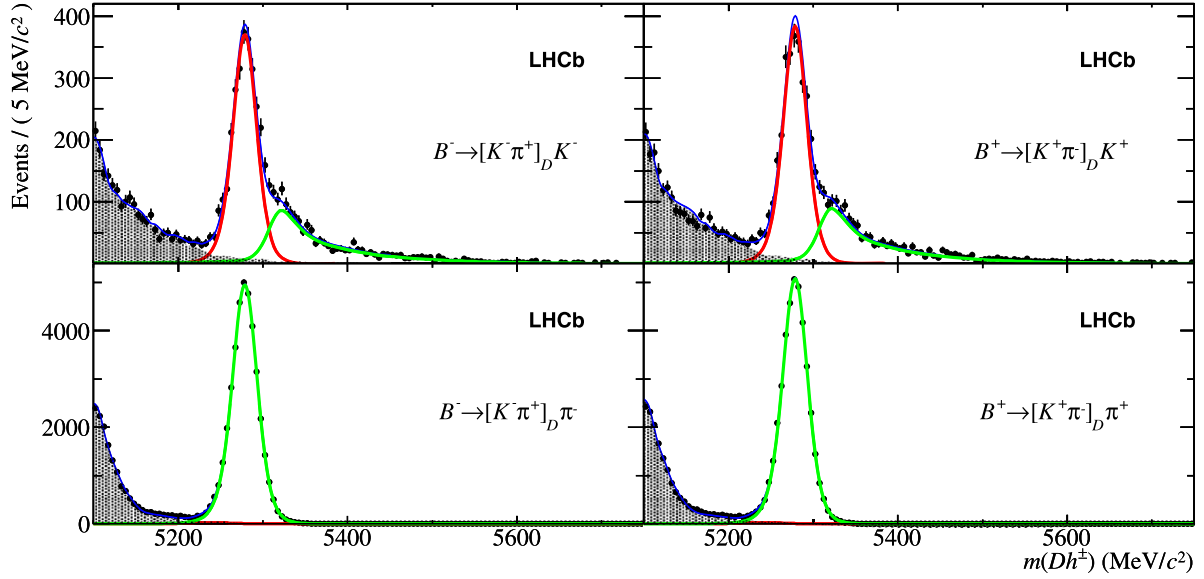


Fig. 1. Invariant mass distributions of selected $B^\pm \rightarrow [K^\pm \pi^\pm]_D h^\pm$ candidates. The left plots are B^- candidates, B^+ are on the right. In the top plots, the bachelor track passes the $DLL_{K\pi} > 4$ cut and the B candidates are reconstructed assigning this track the kaon mass. The remaining events are placed in the sample displayed on the bottom row and are reconstructed with a pion mass hypothesis. The dark (red) curve represents the $B \rightarrow DK^\pm$ events, the light (green) curve is $B \rightarrow D\pi^\pm$. The shaded contribution are partially reconstructed events and the total PDF includes the combinatorial component. (For interpretation of the references to color in this figure legend, the reader is referred to the web version of this Letter.)

$\pm 25 \text{ MeV}/c^2$ of $m_{\text{PDG}}^{D^0}$. This cut is tight enough that no cross feed occurs from the favoured mode into the CP modes. In contrast, the ADS mode suffers a potentially large cross feed from the favoured mode in the circumstance that both D daughters are misidentified ($K \leftrightarrow \pi$). The invariant mass spectrum of such cross feed is broad but peaks around $m_{\text{PDG}}^{D^0}$. It is reduced by vetoing any ADS candidate whose D candidate mass under the exchange of its daughter track mass hypotheses, lies within $\pm 15 \text{ MeV}/c^2$ of $m_{\text{PDG}}^{D^0}$. Importantly for the measurements of R_h^\pm , this veto is also applied to the favoured mode. With the D mass selection and the D daughter PID requirements, this veto reduces the rate of cross feed to an almost negligible rate of $(6 \pm 3) \times 10^{-5}$.

Partially reconstructed events populate the invariant mass region below the B^\pm mass. Such events may enter the signal region, especially where Cabibbo-favoured $B \rightarrow XD\pi^\pm$ modes are misidentified as $B \rightarrow XDK^\pm$. The large simulated sample of inclusive $B_q \rightarrow DX$ decays, $q \in \{u, d, s\}$, is used to model this background. After applying the selection, two non-parametric PDFs [22] are defined (for the $D\pi^\pm$ and DK^\pm selections) and used in the signal extraction fit. These PDFs are applied to all four D modes though two additional contributions are needed in specific cases. In the $D \rightarrow K^+ K^-$ mode, $\Lambda_b^0 \rightarrow [p^+ K^- \pi^+]_{\Lambda_c} h^-$ enters if the pion is missed and the proton is reconstructed as a kaon. In the $B^\pm \rightarrow D_{\text{ADS}} K^\pm$ mode, partially reconstructed $\bar{B}_s^0 \rightarrow D^0 K^+ \pi^-$ decays represent an important, Cabibbo-favoured background. PDFs of both these sources are defined from simulation, smeared by the modest degradation in resolution observed in data. When discussing these contributions, inclusion of the charge conjugate process is implied throughout.

3. Signal yield determination

The observables of interest are determined with a binned maximum-likelihood fit to the invariant mass distributions of selected B candidates [23]. Sensitivity to CP asymmetries is achieved by separating the candidates into B^- and B^+ samples. $B^\pm \rightarrow DK^\pm$ events are distinguished from $B^\pm \rightarrow D\pi^\pm$ using a PID cut on the $DLL_{K\pi}$ of the bachelor track. Events passing this cut are recon-

structed as DK^\pm , events failing the cut are reconstructed as the $D\pi^\pm$ final state. The fit therefore comprises four subsamples — $(B^+, B^-) \times (DK, D\pi)$ — for each D mode, fitted simultaneously and displayed in Figs. 1–4. The total PDF is built from four or five components representing the various sources of events in each subsample.

1. $B^\pm \rightarrow D\pi^\pm$: In the sample failing the bachelor PID cut, a modified Gaussian function,

$$f(x) \propto \exp\left(\frac{-(x - \mu)^2}{2\sigma^2 + (x - \mu)^2 \alpha_{L,R}}\right) \quad (5)$$

describes the asymmetric peak of mean μ and width σ where $\alpha_L (x < \mu)$ and $\alpha_R (x > \mu)$ parameterise the tails.

True $B^\pm \rightarrow D\pi^\pm$ events that pass the PID cut are reconstructed as $B^\pm \rightarrow DK^\pm$. As these events have an incorrect mass assignment they form a displaced mass peak with a tail that extends to higher invariant mass. These events are modelled by the sum of two Gaussian PDFs also altered to include tail components. All parameters are allowed to vary except the lower-mass tail which is fixed to ensure fit stability and later considered amongst the systematic uncertainties. These shapes are considered identical for B^- and B^+ decays and for all four D modes. This assumption is validated with simulation.

2. $B^\pm \rightarrow DK^\pm$: In the sample that passes the $DLL_{K\pi}$ cut on the bachelor, the same modified Gaussian function is used. The mean and the two tail parameters are identical to those of the larger, $B^\pm \rightarrow D\pi^\pm$ peak. The width is 0.95 ± 0.02 times the $D\pi^\pm$ width, as determined by a standalone study of the favoured mode. Its applicability to the CP modes is checked with simulation, assigning an additional systematic uncertainty of 0.01. Events failing the PID cut are described by a fixed shape that is obtained from simulation and later varied to assess the systematic error.
3. Partially reconstructed $B \rightarrow DX$: A fixed, non-parametric PDF, derived from simulation, is used for all subsamples. The yield in each subsample varies independently, making no assumption of CP symmetry.

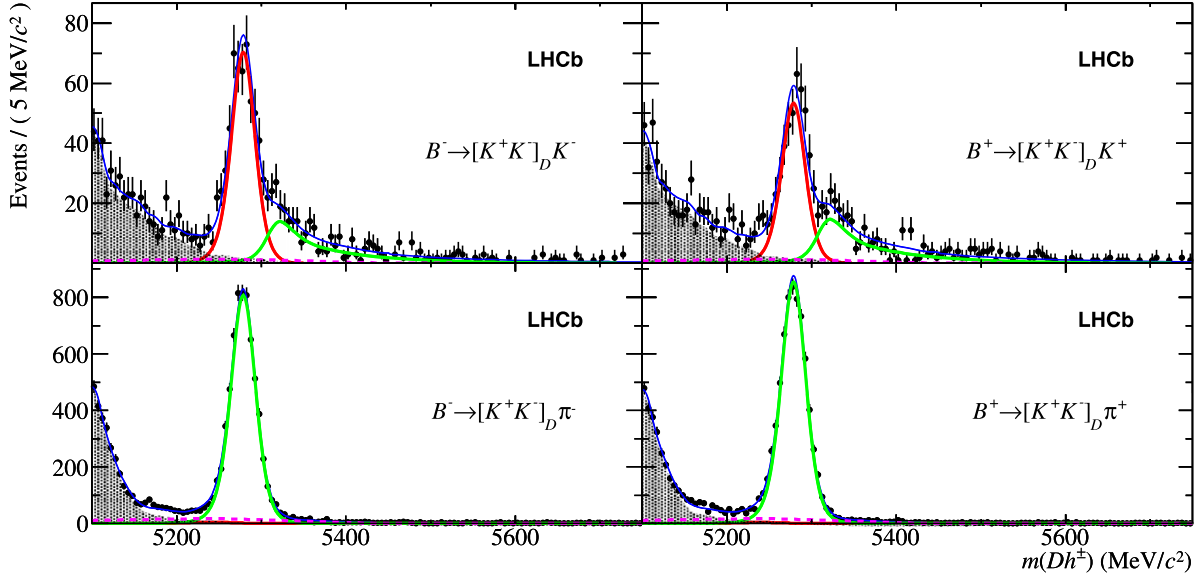


Fig. 2. Invariant mass distributions of selected $B^\pm \rightarrow [K^+K^-]_D h^\pm$ candidates. See the caption of Fig. 1 for a full description. The contribution from $\Lambda_b \rightarrow \Lambda_c^\pm h^\mp$ decays is indicated by the dashed line.

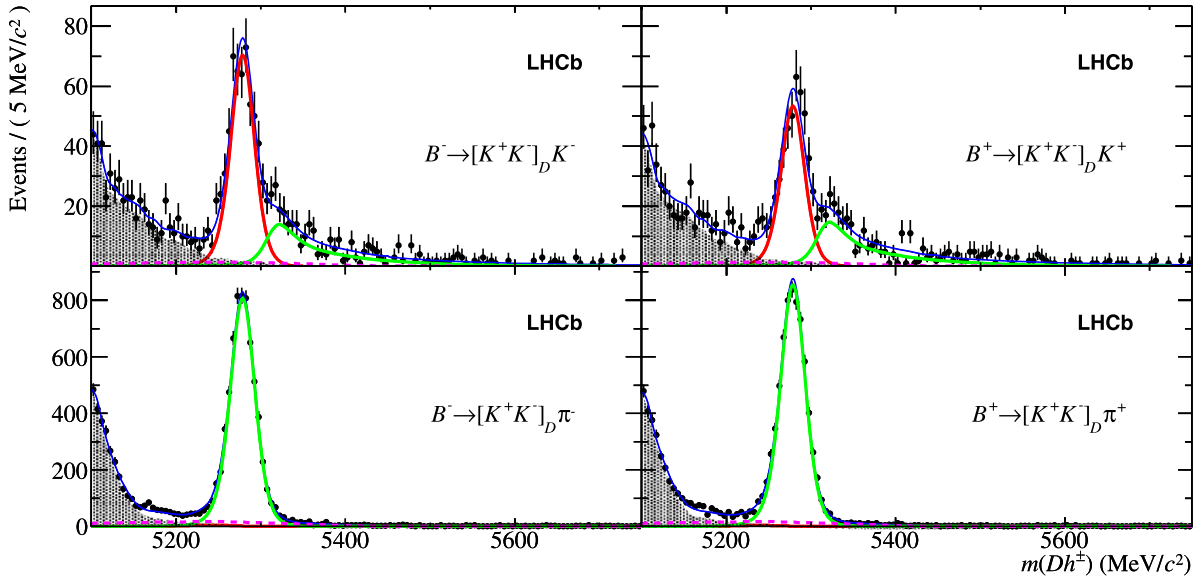


Fig. 3. Invariant mass distributions of selected $B^\pm \rightarrow [\pi^+\pi^-]_D h^\pm$ candidates. See the caption of Fig. 1 for a full description.

4. **Combinatoric background:** A linear approximation is adequate to describe the slope across the invariant mass spectrum considered. A common slope is used in all subsamples, though yields vary independently.
5. **Mode-specific backgrounds:** In the $D \rightarrow KK$ mode, two extra components are used to model $\Lambda_b^0 \rightarrow \Lambda_c^+ h^-$ decays. Though the total contribution is allowed to vary, the shape and relative proportion of $\Lambda_c^+ K^-$ and $\Lambda_c^+ \pi^-$ are fixed. This latter quantity is estimated at 0.060 ± 0.015 , similar to the effective Cabibbo suppression observed in B mesons. For the $B^\pm \rightarrow D_{\text{ADS}} K^\pm$ mode, the shape of the $\bar{B}_s^0 \rightarrow D^0 K^+ \pi^-$ background is taken from simulation. In the fit, this yield is allowed to vary though the reported yield is consistent with the simulated expectation, as derived from the branching fraction [24] and the $b\bar{b}$ hadronisation [25].

The proportion of $B^\pm \rightarrow Dh^\pm$ passing or failing the PID requirement is determined from a calibration analysis of a large sample of $D^{\pm\pm}$ decays reconstructed as $D^{*\pm} \rightarrow D\pi^\pm$, $D \rightarrow K^\mp \pi^\pm$. In this calibration sample, the K and π tracks may be identified, with high purity, using only kinematic variables. This facilitates a measurement of the RICH-based PID efficiency as a function of track momentum, pseudorapidity and number of tracks in the detector. By reweighting the calibration spectra in these variables to match the events in the $B^\pm \rightarrow D\pi^\pm$ peak, the effective PID efficiency of the signal is deduced. This data-driven technique finds a retention rate, for a cut of $\text{DLL}_{K\pi} > 4$ on the bachelor track, of 87.6% and 3.8% for kaons and pions, respectively. A 1.0% systematic uncertainty on the kaon efficiency is estimated from simulation. The $B^\pm \rightarrow D\pi^\pm$ fit to data becomes visibly distorted with variations to the fixed PID efficiency

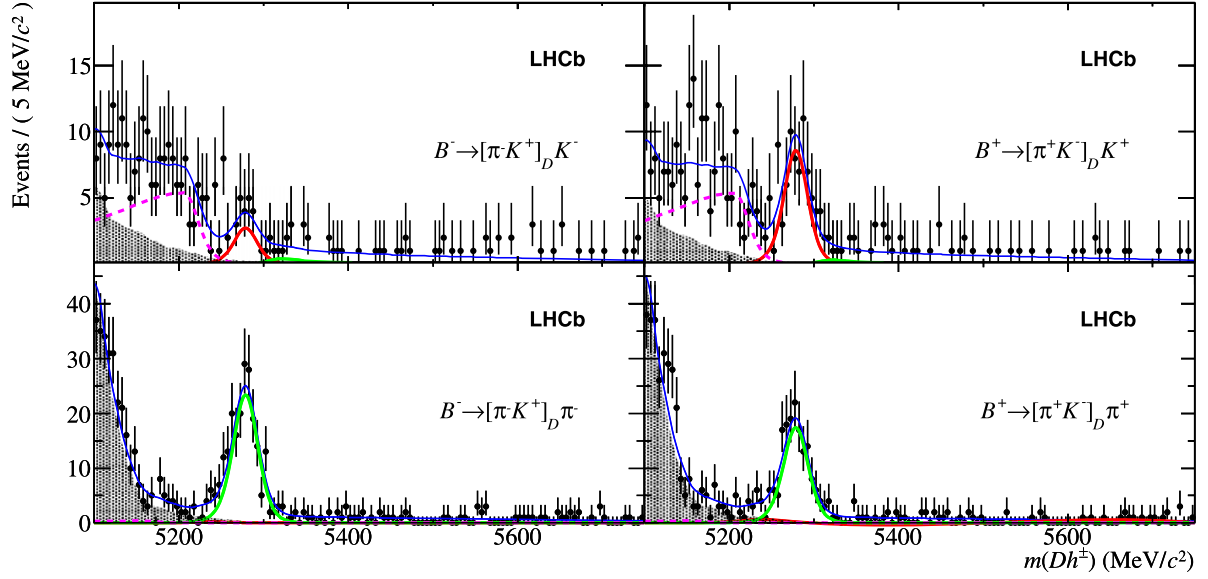


Fig. 4. Invariant mass distributions of selected $B^\pm \rightarrow [\pi^\pm K^\mp]_D h^\pm$ candidates. See the caption of Fig. 1 for a full description. The dashed line here represents the partially reconstructed, but Cabibbo favoured, $B_s^0 \rightarrow \bar{D}^0 K^- \pi^+$ and $\bar{B}_s^0 \rightarrow D^0 K^+ \pi^-$ decays where the pions are lost. The pollution from favoured mode cross feed is drawn, but is too small to be seen.

Table 1

Corrected event yields.

B^\pm mode	D mode	B^-	B^+
DK^\pm	$K^\pm \pi^\mp$	3170 ± 83	3142 ± 83
	$K^\pm K^\mp$	592 ± 40	439 ± 30
	$\pi^\pm \pi^\mp$	180 ± 22	137 ± 16
	$\pi^\pm K^\mp$	23 ± 7	73 ± 11
$D\pi^\pm$	$K^\pm \pi^\mp$	40767 ± 310	40774 ± 310
	$K^\pm K^\mp$	6539 ± 129	6804 ± 135
	$\pi^\pm \pi^\mp$	1969 ± 69	1973 ± 69
	$\pi^\pm K^\mp$	191 ± 16	143 ± 14

$> \pm 0.2\%$ so this value is taken as the systematic uncertainty for pions.

A small negative asymmetry (defined in the same sense as Eq. (2)) is expected in the detection of K^- and K^+ mesons due to their different interaction lengths. A fixed value of $(-0.5 \pm 0.7)\%$ is assigned for each occurrence of strangeness in the final state. The equivalent asymmetry for pions is expected to be much smaller and $(0.0 \pm 0.7)\%$ is assigned. This uncertainty also accounts for the residual physical asymmetry between the left and right sides of the detector after summing both magnet-polarity datasets. Simulation of B meson production in pp collisions suggests a small excess of B^+ over B^- mesons. A production asymmetry of $(-0.8 \pm 0.7)\%$ is assumed in the fit such that the combination of these estimates aligns with the observed raw asymmetry of $B^\pm \rightarrow J/\psi K^\pm$ decays at LHCb [26]. Ongoing studies of these instrumentation asymmetries will reduce the associated systematic uncertainty in future analyses.

The final $B^\pm \rightarrow Dh^\pm$ signal yields, after summing the events that pass and fail the bachelor PID cut, are shown in Table 1. The invariant mass spectra of all 16 $B^\pm \rightarrow [h^+ h^-]_D h^\pm$ modes are shown in Figs. 1–4. Regarding the $B^\pm \rightarrow D\pi^\pm$ mass resolution: respectively, 14.1 ± 0.1 , 14.2 ± 0.1 and 14.2 ± 0.2 MeV/ c^2 are found for the $D \rightarrow KK$, $K\pi$ and $\pi\pi$ modes with common tail parameters $\alpha_L = 0.115 \pm 0.003$ and $\alpha_R = 0.083 \pm 0.002$. As explained above, the $B^\pm \rightarrow DK^\pm$ widths are fixed relative to these values.

The ratio of partial widths relates to the ratio of event yields by the relative efficiency with which $B^\pm \rightarrow DK^\pm$ and $B^\pm \rightarrow D\pi^\pm$

Table 2

Systematic uncertainties on the observables. PID refers to the fixed efficiency of the $DLL_{K\pi}$ cut on the bachelor track. PDFs refers to the variations of the fixed shapes in the fit. “Sim” refers to the use of simulation to estimate relative efficiencies of the signal modes which includes the branching fraction estimates of the Λ_b^0 background. $A_{\text{instr.}}$ quantifies the uncertainty on the production, interaction and detection asymmetries.

$\times 10^{-3}$	PID	PDFs	Sim	$A_{\text{instr.}}$	Total
$R_{K\pi}^{K\pi}$	1.4	0.9	0.8	0	1.8
$R_{K\pi}^{KK}$	1.3	0.8	0.9	0	1.8
$R_{K\pi}^{K\pi}$	1.3	0.6	0.8	0	1.7
$A_{K\pi}^{K\pi}$	0	1.0	0	9.4	9.5
$A_{K\pi}^{KK}$	0.2	4.1	0	16.9	17.4
$A_{K\pi}^{KK}$	1.6	1.3	0.5	9.5	9.7
$A_{K\pi}^{\pi\pi}$	1.9	2.3	0	9.0	9.5
$A_{K\pi}^{K\pi}$	0.1	6.6	0	9.5	11.6
$A_{K\pi}^{\pi\pi}$	0.1	0.4	0	9.9	9.9
R_K^-	0.2	0.4	0	0.1	0.4
R_K^+	0.4	0.5	0	0.1	0.7
R_π^-	0.01	0.03	0	0.07	0.08
R_π^+	0.01	0.03	0	0.07	0.07

decays are reconstructed. This ratio, estimated from simulation, is 1.012, 1.009 and 1.005 for $D \rightarrow KK$, $K\pi$, $\pi\pi$ respectively. A 1.1% systematic uncertainty accounts for the imperfect modelling of the relative pion and kaon absorption in the tracking material, though no evidence of large imperfections are seen.

The fit is constructed such that the observables of interest are parameters of the fit and all systematic uncertainties discussed above enter the fit as constant numbers in the model. To evaluate the effect of these systematic uncertainties, the fit is rerun many times varying each of the systematic constants by its uncertainty. The resulting spread (RMS) in the value of each observable is taken as the systematic uncertainty on that quantity and is summarised in Table 2. Correlations between the uncertainties are considered negligible so the total systematic uncertainty is just the sum in quadrature. For the ratios of partial widths in the favoured and CP modes, the uncertainties on the PID efficiency and the relative width of the DK^\pm and $D\pi^\pm$ peaks dominate. These sources

also contribute in the ADS modes, though the assumed shape of the $\bar{B}_s^0 \rightarrow D^0 K^+ \pi^-$ background is the largest source of systematic uncertainty in the $B^\pm \rightarrow D_{\text{ADS}} K^\pm$ case. For the CP asymmetries, instrumentation asymmetries at LHCb are the largest source of uncertainty.

4. Results

The results of the fit with their statistical uncertainties and assigned systematic uncertainties are:

$$\begin{aligned} R_{K/\pi}^{K\pi} &= 0.0774 \pm 0.0012 \pm 0.0018, \\ R_{K/\pi}^{KK} &= 0.0773 \pm 0.0030 \pm 0.0018, \\ R_{K/\pi}^{\pi\pi} &= 0.0803 \pm 0.0056 \pm 0.0017, \\ A_{\pi}^{K\pi} &= -0.0001 \pm 0.0036 \pm 0.0095, \\ A_K^{K\pi} &= 0.0044 \pm 0.0144 \pm 0.0174, \\ A_K^{KK} &= 0.148 \pm 0.037 \pm 0.010, \\ A_K^{\pi\pi} &= 0.135 \pm 0.066 \pm 0.010, \\ A_{\pi}^{KK} &= -0.020 \pm 0.009 \pm 0.012, \\ A_{\pi}^{\pi\pi} &= -0.001 \pm 0.017 \pm 0.010, \\ R_K^- &= 0.0073 \pm 0.0023 \pm 0.0004, \\ R_K^+ &= 0.0232 \pm 0.0034 \pm 0.0007, \\ R_{\pi}^- &= 0.00469 \pm 0.00038 \pm 0.00008, \\ R_{\pi}^+ &= 0.00352 \pm 0.00033 \pm 0.00007. \end{aligned}$$

From these measurements, the following quantities can be deduced:

$$\begin{aligned} R_{CP+} &\approx \langle R_{K/\pi}^{KK}, R_{K/\pi}^{\pi\pi} \rangle / R_{K/\pi}^{K\pi} \\ &= 1.007 \pm 0.038 \pm 0.012, \\ A_{CP+} &= \langle A_K^{KK}, A_K^{\pi\pi} \rangle \\ &= 0.145 \pm 0.032 \pm 0.010, \\ R_{\text{ADS}(K)} &= (R_K^- + R_K^+)/2 \\ &= 0.0152 \pm 0.0020 \pm 0.0004, \\ A_{\text{ADS}(K)} &= (R_K^- - R_K^+)/ (R_K^- + R_K^+) \\ &= -0.52 \pm 0.15 \pm 0.02, \\ R_{\text{ADS}(\pi)} &= (R_{\pi}^- + R_{\pi}^+)/2 \\ &= 0.00410 \pm 0.00025 \pm 0.00005, \\ A_{\text{ADS}(\pi)} &= (R_{\pi}^- - R_{\pi}^+)/ (R_{\pi}^- + R_{\pi}^+) \\ &= 0.143 \pm 0.062 \pm 0.011, \end{aligned}$$

where the correlations between systematic uncertainties are taken into account in the combination and angled brackets indicate weighted averages. The above definition of R_{CP+} is only approximate and is used for experimental convenience. It assumes the absence of CP violation in $B^\pm \rightarrow D\pi^\pm$ and the favoured $B^\pm \rightarrow DK^\pm$ modes. The exact definition of R_{CP+} is

$$\frac{\Gamma(B^- \rightarrow D_{CP+} K^-) + \Gamma(B^+ \rightarrow D_{CP+} K^+)}{\Gamma(B^- \rightarrow D^0 K^-)} \quad (6)$$

so an additional, and dominant, 1% systematic uncertainty accounts for the approximation. For the same reason, a small addition to the systematic uncertainty of $R_{K/\pi}^{K\pi}$ is needed to quote this result as the ratio of B^\pm branching fractions,

$$\frac{\mathcal{B}(B^- \rightarrow D^0 K^-)}{\mathcal{B}(B^- \rightarrow D^0 \pi^-)} = (7.74 \pm 0.12 \pm 0.19)\%.$$

To summarise, the $B^\pm \rightarrow DK^\pm$ ADS mode is observed with $\sim 10\sigma$ statistical significance when comparing the maximum likelihood to that of the null hypothesis. This mode displays evidence (4.0σ) of a large negative asymmetry, consistent with the asymmetries reported by previous experiments [10–12]. The $B^\pm \rightarrow D\pi^\pm$ ADS mode shows a hint of a positive asymmetry with 2.4σ significance. The KK and $\pi\pi$ modes both show positive asymmetries. The statistical significance of the combined asymmetry, A_{CP+} , is 4.5σ which is similar to that reported in [7,9] albeit with a smaller central value. All these results contain dependence on the weak phase γ and will form an important contribution to a future measurement of this parameter.

Assuming the CP -violating effects in the CP and ADS modes are due to the same phenomenon (namely the interference of $b \rightarrow c\bar{u}s$ and $b \rightarrow u\bar{c}s$ transitions) we compare the maximum likelihood with that under the null-hypothesis in all three D final states where the bachelor is a kaon. This log-likelihood difference is diluted by the non-negligible systematic uncertainties in A_{CP+} and $A_{\text{ADS}(K)}$ which are dominated by the instrumentation asymmetries and hence are highly correlated. In conclusion, with a total significance of 5.8σ , direct CP violation in $B^\pm \rightarrow DK^\pm$ decays is observed.

Acknowledgements

We express our gratitude to our colleagues in the CERN accelerator departments for the excellent performance of the LHC. We thank the technical and administrative staff at CERN and at the LHCb institutes, and acknowledge support from the National Agencies: CAPES, CNPq, FAPERJ and FINEP (Brazil); CERN; NSFC (China); CNRS/IN2P3 (France); BMBF, DFG, HGF and MPG (Germany); SFI (Ireland); INFN (Italy); FOM and NWO (The Netherlands); SCSR (Poland); ANCS (Romania); MinES of Russia and Rosatom (Russia); MICINN, XuntaGal and GENCAT (Spain); SNSF and SER (Switzerland); NAS Ukraine (Ukraine); STFC (United Kingdom); NSF (USA). We also acknowledge the support received from the ERC under FP7 and the Region Auvergne.

Open access

This article is published Open Access at sciencedirect.com. It is distributed under the terms of the Creative Commons Attribution License 3.0, which permits unrestricted use, distribution, and reproduction in any medium, provided the original authors and source are credited.

References

- [1] N. Cabibbo, Phys. Rev. Lett. 10 (1963) 531;
M. Kobayashi, T. Maskawa, Prog. Theor. Phys. 49 (1973) 652.
- [2] C. Jarlskog, Phys. Rev. Lett. 55 (1985) 1039.
- [3] BaBar Collaboration, B. Aubert, et al., Phys. Rev. Lett. 87 (2001) 091801, arXiv:hep-ex/0107013;
Belle Collaboration, K. Abe, et al., Phys. Rev. Lett. 87 (2001) 091802, arXiv:hep-ex/0107061.
- [4] CKMfitter Group, J. Charles, et al., Phys. Rev. D 84 (2011) 033005;
UTfit Collaboration, M. Bona, et al., JHEP 0507 (2005) 028, arXiv:hep-ph/0501199.
- [5] M. Gronau, D. London, Phys. Lett. B 253 (1991) 483;
M. Gronau, D. Wyler, Phys. Lett. B 265 (1991) 172.

- [6] D. Atwood, I. Dunietz, A. Soni, Phys. Rev. Lett. 78 (1997) 3257, arXiv:hep-ph/9612433;
- [7] D. Atwood, I. Dunietz, A. Soni, Phys. Rev. D 63 (2001) 036005, arXiv:hep-ph/0008090.
- [8] Belle Collaboration, K. Abe, et al., Phys. Rev. D 73 (2006) 051106, arXiv:hep-ex/0601032.
- [9] CDF Collaboration, T. Aaltonen, et al., Phys. Rev. D 81 (2010) 031105, arXiv:0911.0425.
- [10] Belle Collaboration, Y. Horii, et al., Phys. Rev. Lett. 106 (2011) 231803, arXiv:1103.5951.
- [11] BaBar Collaboration, P. del Amo Sanchez, et al., Phys. Rev. D 82 (2010) 072006, arXiv:1006.4241.
- [12] CDF Collaboration, T. Aaltonen, et al., Phys. Rev. D 84 (2011) 091504, arXiv:1108.5765.
- [13] BaBar Collaboration, P. del Amo Sanchez, et al., Phys. Rev. Lett. 105 (2010) 121801, arXiv:1005.1096.
- [14] Belle Collaboration, A. Poluektov, et al., Phys. Rev. D 81 (2010) 112002, arXiv:1003.3360.
- [15] LHCb Collaboration, A.A. Alves Jr., et al., JINST 3 (2008) S08005.
- [16] T. Sjöstrand, S. Mrenna, P. Skands, JHEP 0605 (2006) 026, arXiv:hep-ph/0603175.
- [17] D.J. Lange, Nucl. Instrum. Meth. A 462 (2001) 152.
- [18] GEANT4 Collaboration, S. Agostinelli, et al., Nucl. Instrum. Meth. A 506 (2003) 250.
- [19] W.D. Hulsbergen, Nucl. Instrum. Meth. Phys. Res. A 552 (2005) 566, arXiv:physics/0503191.
- [20] Particle Data Group, K. Nakamura, et al., J. Phys. G 37 (2010) 075021.
- [21] A. Hoecker, et al., PoS ACAT (2007) 040, arXiv:physics/0703039, 2007.
- [22] K. Cranmer, Comput. Phys. Commun. 136 (2001) 198, arXiv:hep-ex/0011057.
- [23] W. Verkerke, D. Kirkby, The RooFit toolkit for data modeling, arXiv:physics/0306116.
- [24] LHCb Collaboration, R. Aaij, et al., Phys. Lett. B 706 (2011) 32, arXiv:1110.3676.
- [25] LHCb Collaboration, R. Aaij, et al., Phys. Rev. Lett. 107 (2011) 211801, arXiv:1106.4435.
- [26] LHCb Collaboration, R. Aaij, et al., Measurements of the branching fractions and CP asymmetries of $B^\pm \rightarrow J/\psi \pi^\pm$ and $B^\pm \rightarrow \psi(2S) \pi^\pm$ decays, LHCb-PAPER-2011-024.

LHCb Collaboration

R. Aaij³⁸, C. Abellan Beteta^{33,n}, B. Adeva³⁴, M. Adinolfi⁴³, C. Adrover⁶, A. Affolder⁴⁹, Z. Ajaltouni⁵, J. Albrecht³⁵, F. Alessio³⁵, M. Alexander⁴⁸, S. Ali³⁸, G. Alkhazov²⁷, P. Alvarez Cartelle³⁴, A.A. Alves Jr²², S. Amato², Y. Amhis³⁶, J. Anderson³⁷, R.B. Appleby⁵¹, O. Aquines Gutierrez¹⁰, F. Archilli^{18,35}, A. Artamonov³², M. Artuso^{53,35}, E. Aslanides⁶, G. Auriemma^{22,m}, S. Bachmann¹¹, J.J. Back⁴⁵, V. Balagura^{28,35}, W. Baldini¹⁶, R.J. Barlow⁵¹, C. Barschel³⁵, S. Barsuk⁷, W. Barter⁴⁴, A. Bates⁴⁸, C. Bauer¹⁰, Th. Bauer³⁸, A. Bay³⁶, I. Bediaga¹, S. Belogurov²⁸, K. Belous³², I. Belyaev²⁸, E. Ben-Haim⁸, M. Benayoun⁸, G. Bencivenni¹⁸, S. Benson⁴⁷, J. Benton⁴³, R. Bernet³⁷, M.-O. Bettler¹⁷, M. van Beuzekom³⁸, A. Bien¹¹, S. Bifani¹², T. Bird⁵¹, A. Bizzeti^{17,h}, P.M. Bjørnstad⁵¹, T. Blake³⁵, F. Blanc³⁶, C. Blanks⁵⁰, J. Blouw¹¹, S. Blusk⁵³, A. Bobrov³¹, V. Bocci²², A. Bondar³¹, N. Bondar²⁷, W. Bonivento¹⁵, S. Borghi^{48,51}, A. Borgia⁵³, T.J.V. Bowcock⁴⁹, C. Bozzi¹⁶, T. Brambach⁹, J. van den Brand³⁹, J. Bressieux³⁶, D. Brett⁵¹, M. Britsch¹⁰, T. Britton⁵³, N.H. Brook⁴³, H. Brown⁴⁹, K. de Bruyn³⁸, A. Büchler-Germann³⁷, I. Burducea²⁶, A. Bursche³⁷, J. Buytaert³⁵, S. Cadeddu¹⁵, O. Callot⁷, M. Calvi^{20,j}, M. Calvo Gomez^{33,n}, A. Camboni³³, P. Campana^{18,35}, A. Carbone¹⁴, G. Carboni^{21,k}, R. Cardinale^{19,35,i}, A. Cardini¹⁵, L. Carson⁵⁰, K. Carvalho Akiba², G. Casse⁴⁹, M. Cattaneo³⁵, Ch. Cauet⁹, M. Charles⁵², Ph. Charpentier³⁵, N. Chiapolini³⁷, K. Ciba³⁵, X. Cid Vidal³⁴, G. Ciezarek⁵⁰, P.E.L. Clarke^{47,35}, M. Clemencic³⁵, H.V. Cliff⁴⁴, J. Closier³⁵, C. Coca²⁶, V. Coco³⁸, J. Cogan⁶, P. Collins³⁵, A. Comerma-Montells³³, A. Contu⁵², A. Cook⁴³, M. Coombes⁴³, G. Corti³⁵, B. Couturier³⁵, G.A. Cowan³⁶, R. Currie⁴⁷, C. D'Ambrosio³⁵, P. David⁸, P.N.Y. David³⁸, I. De Bonis⁴, S. De Capua^{21,k}, M. De Cian³⁷, J.M. De Miranda¹, L. De Paula², P. De Simone¹⁸, D. Decamp⁴, M. Deckenhoff⁹, H. Degaudenzi^{36,35}, L. Del Buono⁸, C. Deplano¹⁵, D. Derkach^{14,35}, O. Deschamps⁵, F. Dettori³⁹, J. Dickens⁴⁴, H. Dijkstra³⁵, P. Diniz Batista¹, F. Domingo Bonal^{33,n}, S. Donleavy⁴⁹, F. Dordei¹¹, A. Dosil Suárez³⁴, D. Dossett⁴⁵, A. Dovbnya⁴⁰, F. Dupertuis³⁶, R. Dzhelyadin³², A. Dziurda²³, S. Easo⁴⁶, U. Egede⁵⁰, V. Egorychev²⁸, S. Eidelman³¹, D. van Eijk³⁸, F. Eisele¹¹, S. Eisenhardt⁴⁷, R. Ekelhof⁹, L. Eklund⁴⁸, Ch. Elsasser³⁷, D. Elsby⁴², D. Esperante Pereira³⁴, A. Falabella^{16,14,e}, C. Färber¹¹, G. Fardell⁴⁷, C. Farinelli³⁸, S. Farry¹², V. Fave³⁶, V. Fernandez Albor³⁴, M. Ferro-Luzzi³⁵, S. Filippov³⁰, C. Fitzpatrick⁴⁷, M. Fontana¹⁰, F. Fontanelli^{19,i}, R. Forty³⁵, O. Francisco², M. Frank³⁵, C. Frei³⁵, M. Frosini^{17,f}, S. Furcas²⁰, A. Gallas Torreira³⁴, D. Galli^{14,c}, M. Gandelman², P. Gandini⁵², Y. Gao³, J.-C. Garnier³⁵, J. Garofoli⁵³, J. Garra Tico⁴⁴, L. Garrido³³, D. Gascon³³, C. Gaspar³⁵, R. Gauld⁵², N. Gauvin³⁶, M. Gersabeck³⁵, T. Gershon^{45,35}, Ph. Ghez⁴, V. Gibson⁴⁴, V.V. Gligorov³⁵, C. Göbel⁵⁴, D. Golubkov²⁸, A. Golutvin^{50,28,35}, A. Gomes², H. Gordon⁵², M. Grabalosa Gándara³³, R. Graciani Diaz³³, L.A. Granado Cardoso³⁵, E. Graugés³³, G. Graziani¹⁷, A. Grecu²⁶, E. Greening⁵², S. Gregson⁴⁴, B. Gui⁵³, E. Gushchin³⁰, Yu. Guz³², T. Gys³⁵, C. Hadjivasiliou⁵³, G. Haefeli³⁶, C. Haen³⁵, S.C. Haines⁴⁴, T. Hampson⁴³, S. Hansmann-Menzemer¹¹, R. Harji⁵⁰, N. Harnew⁵², J. Harrison⁵¹, P.F. Harrison⁴⁵, T. Hartmann⁵⁵, J. He⁷, V. Heijne³⁸, K. Hennessy⁴⁹, P. Henrard⁵, J.A. Hernando Morata³⁴, E. van Herwijnen³⁵, E. Hicks⁴⁹, K. Holubyev¹¹, P. Hopchev⁴, W. Hulsbergen³⁸, P. Hunt⁵², T. Huse⁴⁹, R.S. Huston¹², D. Hutchcroft⁴⁹, D. Hynds⁴⁸,

V. Iakovenko⁴¹, P. Ilten¹², J. Imong⁴³, R. Jacobsson³⁵, A. Jaeger¹¹, M. Jahjah Hussein⁵, E. Jans³⁸, F. Jansen³⁸, P. Jaton³⁶, B. Jean-Marie⁷, F. Jing³, M. John^{52,*}, D. Johnson⁵², C.R. Jones⁴⁴, B. Jost³⁵, M. Kaballo⁹, S. Kandybei⁴⁰, M. Karacson³⁵, T.M. Karbach⁹, J. Keaveney¹², I.R. Kenyon⁴², U. Kerzel³⁵, T. Ketel³⁹, A. Keune³⁶, B. Khanji⁶, Y.M. Kim⁴⁷, M. Knecht³⁶, R.F. Koopman³⁹, P. Koppenburg³⁸, M. Korolev²⁹, A. Kozlinskiy³⁸, L. Kravchuk³⁰, K. Kreplin¹¹, M. Kreps⁴⁵, G. Krocker¹¹, P. Krokovny¹¹, F. Kruse⁹, K. Kruzelecki³⁵, M. Kucharczyk^{20,23,35,j}, V. Kudryavtsev³¹, T. Kvaratskheliya^{28,35}, V.N. La Thi³⁶, D. Lacarrere³⁵, G. Lafferty⁵¹, A. Lai¹⁵, D. Lambert⁴⁷, R.W. Lambert³⁹, E. Lanciotti³⁵, G. Lanfranchi¹⁸, C. Langenbruch¹¹, T. Latham⁴⁵, C. Lazzeroni⁴², R. Le Gac⁶, J. van Leerdam³⁸, J.-P. Lees⁴, R. Lefèvre⁵, A. Leflat^{29,35}, J. Lefrançois⁷, O. Leroy⁶, T. Lesiak²³, L. Li³, L. Li Gioi⁵, M. Lieng⁹, M. Liles⁴⁹, R. Lindner³⁵, C. Linn¹¹, B. Liu³, G. Liu³⁵, J. von Loeben²⁰, J.H. Lopes², E. Lopez Asamar³³, N. Lopez-March³⁶, H. Lu³, J. Luisier³⁶, A. Mac Raighne⁴⁸, F. Machefert⁷, I.V. Machikhiliyan^{4,28}, F. Maciuc¹⁰, O. Maev^{27,35}, J. Magnin¹, S. Malde⁵², R.M.D. Mamunur³⁵, G. Manca^{15,d}, G. Mancinelli⁶, N. Mangiafave⁴⁴, U. Marconi¹⁴, R. Märki³⁶, J. Marks¹¹, G. Martellotti²², A. Martens⁸, L. Martin⁵², A. Martín Sánchez⁷, M. Martinelli³⁸, D. Martinez Santos³⁵, A. Massafferri¹, Z. Mathe¹², C. Matteuzzi²⁰, M. Matveev²⁷, E. Maurice⁶, B. Maynard⁵³, A. Mazurov^{16,30,35}, G. McGregor⁵¹, R. McNulty¹², M. Meissner¹¹, M. Merk³⁸, J. Merkel⁹, S. Miglioranza³⁵, D.A. Milanese¹³, M.-N. Minard⁴, J. Molina Rodriguez⁵⁴, S. Monteil⁵, D. Moran¹², P. Morawski²³, R. Mountain⁵³, I. Mous³⁸, F. Muheim⁴⁷, K. Müller³⁷, R. Muresan²⁶, B. Muryn²⁴, B. Muster³⁶, J. Mylroie-Smith⁴⁹, P. Naik⁴³, T. Nakada³⁶, R. Nandakumar⁴⁶, I. Nasteva¹, M. Needham⁴⁷, N. Neufeld³⁵, A.D. Nguyen³⁶, C. Nguyen-Mau^{36,o}, M. Nicol⁷, V. Niess⁵, N. Nikitin²⁹, A. Nomerotski^{52,35}, A. Novoselov³², A. Oblakowska-Mucha²⁴, V. Obraztsov³², S. Oggero³⁸, S. Ogilvy⁴⁸, O. Okhrimenko⁴¹, R. Oldeman^{15,35,d}, M. Orlandea²⁶, J.M. Otalora Goicochea², P. Owen⁵⁰, K. Pal⁵³, J. Palacios³⁷, A. Palano^{13,b}, M. Palutan¹⁸, J. Panman³⁵, A. Papanestis⁴⁶, M. Pappagallo⁴⁸, C. Parkes⁵¹, C.J. Parkinson⁵⁰, G. Passaleva¹⁷, G.D. Patel⁴⁹, M. Patel⁵⁰, S.K. Paterson⁵⁰, G.N. Patrick⁴⁶, C. Patrignani^{19,i}, C. Pavel-Nicorescu²⁶, A. Pazos Alvarez³⁴, A. Pellegrino³⁸, G. Penso^{22,l}, M. Pepe Altarelli³⁵, S. Perazzini^{14,c}, D.L. Perego^{20,j}, E. Perez Trigo³⁴, A. Pérez-Calero Yzquierdo³³, P. Perret⁵, M. Perrin-Terrin⁶, G. Pessina²⁰, A. Petrolini^{19,i}, A. Phan⁵³, E. Picatoste Olloqui³³, B. Pie Valls³³, B. Pietrzyk⁴, T. Pilar⁴⁵, D. Pinci²², R. Plackett⁴⁸, S. Playfer⁴⁷, M. Plo Casasus³⁴, G. Polok²³, A. Poluektov^{45,31}, E. Polcarpo², D. Popov¹⁰, B. Popovici²⁶, C. Potterat³³, A. Powell⁵², J. Prisciandaro³⁶, V. Pugatch⁴¹, A. Puig Navarro³³, W. Qian⁵³, J.H. Rademacker⁴³, B. Rakotomiamanana³⁶, M.S. Rangel², I. Raniuk⁴⁰, G. Raven³⁹, S. Redford⁵², M.M. Reid⁴⁵, A.C. dos Reis¹, S. Ricciardi⁴⁶, A. Richards⁵⁰, K. Rinnert⁴⁹, D.A. Roa Romero⁵, P. Robbe⁷, E. Rodrigues^{48,51}, F. Rodrigues², P. Rodriguez Perez³⁴, G.J. Rogers⁴⁴, S. Roiser³⁵, V. Romanovsky³², M. Rosello^{33,n}, J. Rouvinet³⁶, T. Ruf³⁵, H. Ruiz³³, G. Sabatino^{21,k}, J.J. Saborido Silva³⁴, N. Sagidova²⁷, P. Sail⁴⁸, B. Saitta^{15,d}, C. Salzmann³⁷, M. Sannino^{19,i}, R. Santacesaria²², C. Santamarina Rios³⁴, R. Santinelli³⁵, E. Santovetti^{21,k}, M. Sapunov⁶, A. Sarti^{18,l}, C. Satriano^{22,m}, A. Satta²¹, M. Savrie^{16,e}, D. Savrina²⁸, P. Schaack⁵⁰, M. Schiller³⁹, H. Schindler³⁵, S. Schleich⁹, M. Schlupp⁹, M. Schmelling¹⁰, B. Schmidt³⁵, O. Schneider³⁶, A. Schopper³⁵, M.-H. Schune⁷, R. Schwemmer³⁵, B. Sciascia¹⁸, A. Sciubba^{18,l}, M. Seco³⁴, A. Semennikov²⁸, K. Senderowska²⁴, I. Sepp⁵⁰, N. Serra³⁷, J. Serrano⁶, P. Seyfert¹¹, M. Shapkin³², I. Shapoval^{40,35}, P. Shatalov²⁸, Y. Shcheglov²⁷, T. Shears⁴⁹, L. Shekhtman³¹, O. Shevchenko⁴⁰, V. Shevchenko²⁸, A. Shires⁵⁰, R. Silva Coutinho⁴⁵, T. Skwarnicki⁵³, N.A. Smith⁴⁹, E. Smith^{52,46}, K. Sobczak⁵, F.J.P. Soler⁴⁸, A. Solomin⁴³, F. Soomro^{18,35}, B. Souza De Paula², B. Spaan⁹, A. Sparkes⁴⁷, P. Spradlin⁴⁸, F. Stagni³⁵, S. Stahl¹¹, O. Steinkamp³⁷, S. Stoica²⁶, S. Stone^{53,35}, B. Storaci³⁸, M. Straticiuc²⁶, U. Straumann³⁷, V.K. Subbiah³⁵, S. Swientek⁹, M. Szczekowski²⁵, P. Szczypka³⁶, T. Szumlak²⁴, S. T'Jampens⁴, E. Teodorescu²⁶, F. Teubert³⁵, C. Thomas⁵², E. Thomas³⁵, J. van Tilburg¹¹, V. Tisserand⁴, M. Tobin³⁷, S. Topp-Joergensen⁵², N. Torr⁵², E. Tournefier^{4,50}, S. Tourneur³⁶, M.T. Tran³⁶, A. Tsaregorodtsev⁶, N. Tuning³⁸, M. Ubeda Garcia³⁵, A. Ukleja²⁵, U. Uwer¹¹, V. Vagnoni¹⁴, G. Valenti¹⁴, R. Vazquez Gomez³³, P. Vazquez Regueiro³⁴, S. Vecchi¹⁶, J.J. Velthuis⁴³, M. Veltri^{17,g}, B. Viaud⁷, I. Videau⁷, D. Vieira², X. Vilasis-Cardona^{33,n}, J. Visniakov³⁴, A. Vollhardt³⁷, D. Volyanskyy¹⁰, D. Voong⁴³, A. Vorobyev²⁷, H. Voss¹⁰, R. Waldi⁵⁵, S. Wandernoth¹¹, J. Wang⁵³, D.R. Ward⁴⁴, N.K. Watson⁴², A.D. Webber⁵¹, D. Websdale⁵⁰, M. Whitehead⁴⁵, D. Wiedner¹¹, L. Wiggers³⁸, G. Wilkinson⁵², M.P. Williams^{45,46}, M. Williams⁵⁰, F.F. Wilson⁴⁶, J. Wishahi⁹, M. Witek²³, W. Witzeling³⁵, S.A. Wotton⁴⁴, K. Wyllie³⁵, Y. Xie⁴⁷, F. Xing⁵², Z. Xing⁵³, Z. Yang³, R. Young⁴⁷,

O. Yushchenko³², M. Zangoli¹⁴, M. Zavertyaev^{10,a}, F. Zhang³, L. Zhang⁵³, W.C. Zhang¹², Y. Zhang³,
A. Zhelezov¹¹, L. Zhong³, A. Zvyagin³⁵

- ¹ Centro Brasileiro de Pesquisas Físicas (CBPF), Rio de Janeiro, Brazil
- ² Universidade Federal do Rio de Janeiro (UFRJ), Rio de Janeiro, Brazil
- ³ Center for High Energy Physics, Tsinghua University, Beijing, China
- ⁴ LAPP, Université de Savoie, CNRS/IN2P3, Annecy-Le-Vieux, France
- ⁵ Clermont Université, Université Blaise Pascal, CNRS/IN2P3, LPC, Clermont-Ferrand, France
- ⁶ CPPM, Aix-Marseille Université, CNRS/IN2P3, Marseille, France
- ⁷ LAL, Université Paris-Sud, CNRS/IN2P3, Orsay, France
- ⁸ LPNHE, Université Pierre et Marie Curie, Université Paris Diderot, CNRS/IN2P3, Paris, France
- ⁹ Fakultät Physik, Technische Universität Dortmund, Dortmund, Germany
- ¹⁰ Max-Planck-Institut für Kernphysik (MPIK), Heidelberg, Germany
- ¹¹ Physikalisches Institut, Ruprecht-Karls-Universität Heidelberg, Heidelberg, Germany
- ¹² School of Physics, University College Dublin, Dublin, Ireland
- ¹³ Sezione INFN di Bari, Bari, Italy
- ¹⁴ Sezione INFN di Bologna, Bologna, Italy
- ¹⁵ Sezione INFN di Cagliari, Cagliari, Italy
- ¹⁶ Sezione INFN di Ferrara, Ferrara, Italy
- ¹⁷ Sezione INFN di Firenze, Firenze, Italy
- ¹⁸ Laboratori Nazionali dell'INFN di Frascati, Frascati, Italy
- ¹⁹ Sezione INFN di Genova, Genova, Italy
- ²⁰ Sezione INFN di Milano Bicocca, Milano, Italy
- ²¹ Sezione INFN di Roma Tor Vergata, Roma, Italy
- ²² Sezione INFN di Roma La Sapienza, Roma, Italy
- ²³ Henryk Niewodniczanski Institute of Nuclear Physics Polish Academy of Sciences, Kraków, Poland
- ²⁴ AGH University of Science and Technology, Kraków, Poland
- ²⁵ Soltan Institute for Nuclear Studies, Warsaw, Poland
- ²⁶ Horia Hulubei National Institute of Physics and Nuclear Engineering, Bucharest-Magurele, Romania
- ²⁷ Petersburg Nuclear Physics Institute (PNPI), Gatchina, Russia
- ²⁸ Institute of Theoretical and Experimental Physics (ITEP), Moscow, Russia
- ²⁹ Institute of Nuclear Physics, Moscow State University (SINP MSU), Moscow, Russia
- ³⁰ Institute for Nuclear Research of the Russian Academy of Sciences (INR RAN), Moscow, Russia
- ³¹ Budker Institute of Nuclear Physics (SB RAS) and Novosibirsk State University, Novosibirsk, Russia
- ³² Institute for High Energy Physics (IHEP), Protvino, Russia
- ³³ Universitat de Barcelona, Barcelona, Spain
- ³⁴ Universidad de Santiago de Compostela, Santiago de Compostela, Spain
- ³⁵ European Organization for Nuclear Research (CERN), Geneva, Switzerland
- ³⁶ Ecole Polytechnique Fédérale de Lausanne (EPFL), Lausanne, Switzerland
- ³⁷ Physik-Institut, Universität Zürich, Zürich, Switzerland
- ³⁸ Nikhef National Institute for Subatomic Physics, Amsterdam, The Netherlands
- ³⁹ Nikhef National Institute for Subatomic Physics and Vrije Universiteit, Amsterdam, The Netherlands
- ⁴⁰ NSC Kharkiv Institute of Physics and Technology (NSC KIPT), Kharkiv, Ukraine
- ⁴¹ Institute for Nuclear Research of the National Academy of Sciences (KINR), Kyiv, Ukraine
- ⁴² University of Birmingham, Birmingham, United Kingdom
- ⁴³ H.H. Wills Physics Laboratory, University of Bristol, Bristol, United Kingdom
- ⁴⁴ Cavendish Laboratory, University of Cambridge, Cambridge, United Kingdom
- ⁴⁵ Department of Physics, University of Warwick, Coventry, United Kingdom
- ⁴⁶ STFC Rutherford Appleton Laboratory, Didcot, United Kingdom
- ⁴⁷ School of Physics and Astronomy, University of Edinburgh, Edinburgh, United Kingdom
- ⁴⁸ School of Physics and Astronomy, University of Glasgow, Glasgow, United Kingdom
- ⁴⁹ Oliver Lodge Laboratory, University of Liverpool, Liverpool, United Kingdom
- ⁵⁰ Imperial College London, London, United Kingdom
- ⁵¹ School of Physics and Astronomy, University of Manchester, Manchester, United Kingdom
- ⁵² Department of Physics, University of Oxford, Oxford, United Kingdom
- ⁵³ Syracuse University, Syracuse, NY, United States
- ⁵⁴ Pontifícia Universidade Católica do Rio de Janeiro (PUC-Rio), Rio de Janeiro, Brazil^p
- ⁵⁵ Physikalisches Institut, Universität Rostock, Rostock, Germany^q

* Corresponding author.

E-mail address: malcolm.john@physics.ox.ac.uk (M. John).

^a P.N. Lebedev Physical Institute, Russian Academy of Science (LPI RAS), Moscow, Russia.

^b Università di Bari, Bari, Italy.

^c Università di Bologna, Bologna, Italy.

^d Università di Cagliari, Cagliari, Italy.

^e Università di Ferrara, Ferrara, Italy.

^f Università di Firenze, Firenze, Italy.

^g Università di Urbino, Urbino, Italy.

^h Università di Modena e Reggio Emilia, Modena, Italy.

ⁱ Università di Genova, Genova, Italy.

^j Università di Milano Bicocca, Milano, Italy.

^k Università di Roma Tor Vergata, Roma, Italy.

^l Università di Roma La Sapienza, Roma, Italy.

^m Università della Basilicata, Potenza, Italy.

ⁿ LIFAELS, La Salle, Universitat Ramon Llull, Barcelona, Spain.

^o Hanoi University of Science, Hanoi, Viet Nam.

^p Associated to Universidade Federal do Rio de Janeiro (UFRJ), Rio de Janeiro, Brazil.

^q Associated to Physikalisches Institut, Ruprecht-Karls-Universität Heidelberg, Heidelberg, Germany.